

Numerical analysis of a calibration problem for simulating electric fault arc tests

TORSTEN HEIN, BERND HOFMANN, ARND MEYER AND PETER STEINHORST

Faculty of Mathematics

Chemnitz University of Technology, D-09107 Chemnitz, Germany

email:

thein@mathematik.tu-chemnitz.de

b.hofmann@mathematik.tu-chemnitz.de

a.meyer@mathematik.tu-chemnitz.de

p.steinhorst@mathematik.tu-chemnitz.de

Abstract

In this paper we present a mathematical model and a numerical approach for a computer-based simulation of electric fault arc tests including the solution of corresponding direct and inverse problems. In particular, we replace the complicated initial-boundary value problem of heat transfer in arc tests by a one-dimensional model based on a purely time-dependent temperature function $G(t)$ of hot gas in a neighborhood of the arc. We analyze the forward problem with respect to its well-posedness and suggest an appropriate numerical approximation. However, we are especially interested in the ill-posed nonlinear inverse problem of identifying (calibrating) the important parameter function G from temperature measurements at a defined distance to the arc during some time interval, where a simplified test procedure is exploited for obtaining temperature data. We present a least-squares solution indicating the ill-posedness effect by strong oscillations and compare a solution from Tikhonov regularization with a solution from a descriptive regularization approach.

Keywords: Parameter identification; electric fault arcs; initial-boundary value problems; ill-posedness; regularization

MSC 2000 Subject Classification: 35R30, 65M30, 65J20

1 Introduction

Fault arc tests are performed in textile research and certification of protective clothes. The protective clothes we are concerned with are used by people working on electric installations who are exposed to the risk of fault arc accidents, potentially causing injury with heavy burns. There exist different international standards for arc tests on such

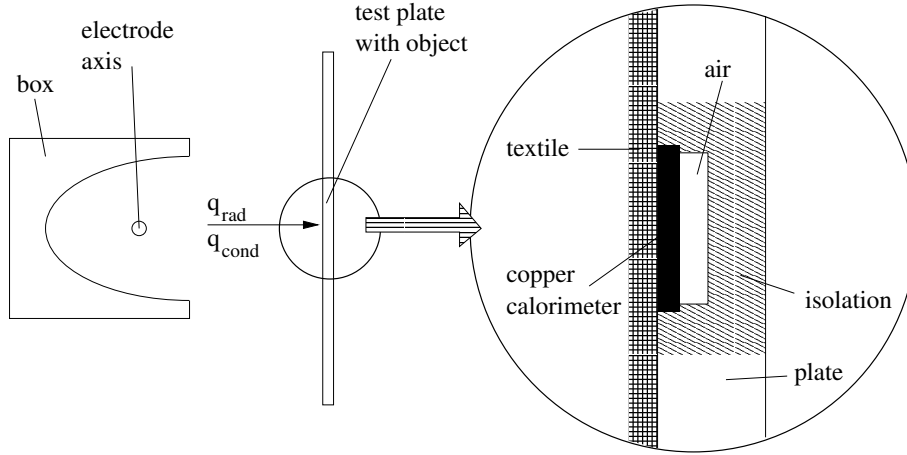


Figure 1: Schematic test arrangement.

protective textiles [9]. One particular European test is the so-called CENELEC test, prescribed in the pre-standard ENV 50354:2001. This box-arc test method [11] contains a visual assessment (after flaming, hole formation, shrinking etc.) as a qualitative criterion and was extended and improved by including additionally a quantitative measurement of temperatures in order to get information about transmitted energy. A schematic test arrangement of such a complemented test is shown in Figure 1.

An electric arc is fired between two vertically arranged electrodes in a test circuit of defined voltage (AC). After the burning-time interval of $t_p = 0.5s$ the arc is switched off. A surrounding box focuses thermal arc effects in direction to a test plate with test object, which is arranged in a defined distance to the electrodes. The object consists of a variable number of textile layers stretched onto the test plate and a skin-simulating copper calorimeter embedded by an isolating block in the test plate as shown in Figure 1. The calorimeter is connected to a thermocouple, and so the calorimeter temperature is measured from the arc ignition ($t = 0$) until the end of measuring time $t^{\text{end}} = 30s$.

Such tests are expensive to realize, and extensive technical equipment is required. A current of 7kA has to be controlled and held stable in a circuit for half a second, the complete arrangement has to sustain temperatures of several thousand degrees. Moreover, the textile or clothing which is tested will be destroyed during the test. For these reasons large series of arc tests, for instance in order to take parametric studies, are not practicable. This gives rise to the need for a model of the test which enables us to study the influence of some material parameters on thermal test results.

A numerical simulation of calorimetric arc effects based on the complemented test method was realized at Chemnitz University of Technology in cooperation with the Saxon Textile Research Institute (STFI) and Ilmenau University of Technology, [12]. The underlying model, proposed in this paper, is based on the following assumptions:

- A nonlinear heat equation is set for the heat flux inside the object (textile and calorimeter). An important part of the nonlinearities takes the radiation which is modelled inside the object by a special source term.

- For modelling the boundary conditions a heat transfer proportional to the temperature difference at the interesting material borders is assumed.
- Both boundary conditions and radiation source include a simulated gas temperature G , modelling the influences of hot gas between the arc and the examined object. Unfortunately, this temperature as function of time is unknown. The reason for this holds in the high, fast changing temperatures and the explosion effects caused by the arc. The used measuring device is not able to determine this temperature (nevertheless, exactly seen G is only a model quantity and so cannot be measured).

Thus, in order to use the model we need the function G . Its determination is proposed in the following manner:

- We focus on a special case, the test without textile layers.
- Temperatures on the back side of the calorimeter can be measured for this test. This way, measurement data is available.
- The determination of the unknown temperature function G by using this data leads to an inverse problem. Studying it in several aspects is the main part of the paper.

This paper, which is an extended version of [13], will be organized as follows: For the numerical simulation of the test we used a mathematical model, which will be described in Section 2. In the model building process we have replaced the very complex structure of the system formed by arc, heated gas and reflecting box by a gas temperature function G depending on time t only. The determination (calibration) of this parameter function G , which influences the result of test simulation in an essential manner, leads to the inverse problem discussed in this paper. Before handling the stable approximate solution of this inverse problem in Sections 5 and 6, we briefly analyze the associated forward problem in Section 3 and discuss its numerical solution in Section 4. We end with some conclusions in Section 7.

2 The mathematical model

We have simplified the whole test arrangement in form of a locally one-dimensional heat equation problem, where the gas temperature near the arc is assumed to be a function $G(t)$ of time t . The spatial x -axis lies orthogonal to the surface of the test object (plate with or without textile) such that the temperature of interest here are directed along the x -axis. Figure 2 shows the modelled object with three textile layers as an example.

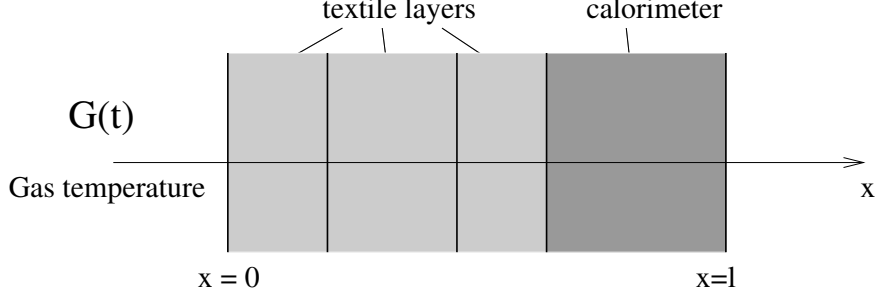


Figure 2: 1D-model of the object.

We use the following notations:

x	1D local coordinate, $x \in (0, l)$,
t	time, $t \in [0, t^{\text{end}}]$,
$u = u(x, t)$	temperature in the object,
$G = G(t)$	temperature of the hot gas,
$C^A(x, t, u)$	apparent heat capacity (modified, specified by volume),
$\kappa(x, u)$	thermal conductivity,
$f_{\text{rad}}(x, t, G, D)$	radiation heat source term,
h_0, h_s	heat transfer coefficients.

The occurring temperatures u and G are seen as relative temperatures with respect to the ambient temperature $T_0 = 300K$. Moreover, we define the space-time cylinder $Q := (0, l) \times (0, t^{\text{end}})$.

Then, the temperature distribution $u = u(x, t)$ is the solution of the initial-boundary value problem for the heat equation

$$C^A(x, t, u) \frac{\partial u}{\partial t} - \frac{\partial}{\partial x} \left(\kappa(x, u) \frac{\partial u}{\partial x} \right) = f_{\text{rad}}(x, t, G(t), u(0, t)), \quad (x, t) \in Q, \quad (1)$$

with boundary conditions

$$-\kappa(0, u(0, t)) \frac{\partial u(0, t)}{\partial x} = h_0(G(t) - u(0, t)), \quad t \in (0, t^{\text{end}}], \quad (2)$$

$$\kappa(l, u(l, t)) \frac{\partial u(l, t)}{\partial x} = -h_s u(l, t), \quad t \in (0, t^{\text{end}}], \quad (3)$$

and initial condition

$$u(x, 0) = 0, \quad x \in [0, l]. \quad (4)$$

Heat effects enter the model by boundary conditions in form of heat convection and by the source term f_{rad} in the differential equation indicating the effect of radiation. We formulate the corresponding forward problem.

Definition 2.1 (Forward problem) *Let the parameters C^A , κ , h_s , h_0 , G and f_{rad} be given. Find a solution u of (1) – (4) in \bar{Q} .*

Note, that the source term contains a special nonlinearity. In particular, f_{rad} depends only on the temperature $u(0, t)$, $t \in [0, t^{\text{end}}]$, at the left boundary. Standard theory of quasilinear differential equations presumes, that f_{rad} is a function of the temperature u itself. Therefore, we briefly consider conditions for the solvability of the problem (1) – (4). We assume for the gas temperature that $G \in \mathcal{D}_{\text{box}}$ with

$$\mathcal{D}_{\text{box}} := \{G \in C[0, t^{\text{end}}] : 0 \leq G(t) \leq G_{\text{max}}, t \in [0, t^{\text{end}}]\}$$

and a given maximal gas temperature G_{max} . Here, $C[0, t^{\text{end}}]$ denotes the Banach space of all continuous functions on the interval $[0, t^{\text{end}}]$. Moreover, for the coefficients C^A and κ we assume for all $(x, t, u) \in \overline{Q} \times \mathbb{R}$ that

$$0 < C_1^A \leq C^A(x, t, u) \leq C_2^A < \infty \quad \text{and} \quad 0 < \kappa_1 \leq \kappa(x, u) \leq \kappa_2 < \infty, \quad (5)$$

with constants C_1^A , C_2^A , κ_1 and κ_2 . Then we can prove the following existence result in the space $C^{2,1}(\overline{Q})$, which contains all functions on $\overline{Q} \subset \mathbb{R}^2$, which are twice continuously differentiable with respect to the first and once continuously differentiable with respect to the second variable.

Proposition 2.2 *Let $G \in \mathcal{D}_{\text{box}}$ and let the inequalities (5) hold. Moreover, we assume that $|f_{\text{rad}}(x, t, G, D)| \leq C$ for all $(x, t) \in \overline{Q}$, $G \in [0, G_{\text{max}}]$, for some constant $C > 0$ and $|D| \leq \tilde{C} \max\{C, G_{\text{max}}\}$ for some constant $\tilde{C} > 0$, which depends on C_i^A, κ_i , $i = 1, 2$ and t^{end} . Then there exists a solution $u \in C^{2,1}(\overline{Q})$ of (1) – (4).*

SKETCH OF A PROOF. We consider the mapping $M : C(\overline{Q}) \rightarrow C(\overline{Q})$, where $M(u_0)$ is the solution of (1) – (4) when u is replaced by u_0 in the coefficients C^A and κ and in the source term f_{rad} . Since we consider a linear parabolic initial boundary value problem, the mapping M is well-defined (see, e.g., [10, Theorem IV.5.4] for an existence and uniqueness result). Moreover, by [10, Theorem I.2.3] we have the estimate

$$\max_{(x,t)} |u(x, t)| \leq C_u := \tilde{C} \max \left\{ \max_{(x,t)} |\tilde{f}(x, t)|, G_{\text{max}} \right\},$$

where $\tilde{f}(x, t) := f_{\text{rad}}(x, t, G(t), u_0(0, t))$ and \tilde{C} depends only on C_i^A, κ_i , $i = 1, 2$ and t^{end} . If we introduce the set $\Omega := \{u \in C(\overline{Q}) : \max |u| \leq C_u \text{ on } \overline{Q}\}$, then M maps Ω into itself. Moreover $M(u_0) \in C^{2,1}(\overline{Q})$ is uniformly bounded in the norm of $C^{2,1}(\overline{Q})$ (see [10, Theorem IV.5.3]). Hence, by the well-known compactness of embedding from $C^{2,1}(\overline{Q})$ into $C(\overline{Q})$, the range $M(\tilde{\Omega})$ for any bounded subset $\tilde{\Omega} \subset \Omega$ is relatively compact in $C(\overline{Q})$. Thus, M is a compact operator. By Schauder's fixed-point theorem (see, e.g., [16, Theorem 2.A]) M contains a fixed-point which solves (1) – (4). ■

Recalling the technical background, the recommended continuity of the function G is not very restrictive with respect to the model.

In order to calculate $u(x, t)$ from (1) – (4) the knowledge of the gas temperature $G(t)$, $t \in [0, t^{\text{end}}]$, is required. For the determination of this function temperature measurement data from calibration tests are used. The calibration test is performed without textile layers, where the object consists of the test plate with the calorimeter only. For this reason, we use the simplified version

$$C_{\text{Cu}} \frac{\partial u}{\partial t} - \frac{\partial}{\partial x} \left(\kappa_{\text{Cu}} \frac{\partial u}{\partial x} \right) = f_{\text{rad}}(x, t, G(t), u(0, t)), \quad (x, t) \in Q, \quad (6)$$

of heat equation. Here the volumetric heat capacity C_{Cu} and the thermal conductivity κ_{Cu} are assumed to be constant. Note that κ_{Cu} in fact depends on the temperature, but the measured and simulated temperatures of the copper calorimeter are from the temperature interval $[20^\circ\text{C}, 110^\circ\text{C}]$ (see Section 6). For this range, however, the thermal conductivity of copper is nearly a constant (see, e.g. [7, Chap. 6-12, Table 6-18]). The radiation source term has the structure

$$f_{\text{rad}}(x, t, G(t), u(0, t)) = \gamma e^{-\gamma x} (q_a(t) + \beta_{\text{Gas}}(G(t) + T_0)^4 - \beta_{\text{Obj}}((u(0, t) + T_0)^4 - T_0^4)) \quad (7)$$

for $(x, t) \in Q$ with positive constants $\beta_{\text{Gas}}, \beta_{\text{Obj}}$ and γ , see e.g. [14]. The function $q_a(t)$ is the given source term of the burning arc, which is a piecewise constant function which vanishes on the interval $(t_p, t^{\text{end}}]$. The boundary conditions (2) – (3) and the initial condition (4) are reduced to

$$\left. \begin{aligned} -\kappa_{\text{Cu}} \frac{\partial u(0, t)}{\partial x} &= h_0(G(t) - u(0, t)), & t \in [0, t^{\text{end}}], \\ \kappa_{\text{Cu}} \frac{\partial u(l, t)}{\partial x} &= -h_s u(l, t), & t \in [0, t^{\text{end}}], \\ u(x, 0) &= 0, & x \in [0, l]. \end{aligned} \right\} \quad (8)$$

In this simplified model nonlinearities occur only in the radiation source term.

The inverse problem under consideration here aims at finding the gas temperature function $G(t)$ from given lateral data $u(l, t)$ for $t \in [0, t^{\text{end}}]$ solving the problem (6) – (8).

Definition 2.3 (Calibration Problem) *Let the parameters $C_{\text{Cu}}, \kappa_{\text{Cu}}, h_0, h_s$ and f_{rad} be given. Find a pair of functions (G, u) such that u is a solution of (6) – (8) on \overline{Q} , which fulfills the equation*

$$u(l, t) = u_{\text{data}}(t), \quad t \in [0, t^{\text{end}}], \quad (9)$$

for a given lateral measurement $u_{\text{data}}(t)$, $t \in [0, t^{\text{end}}]$.

Let $L^2(0, t^{\text{end}})$ be the space of source functions to be determined. Furthermore, let $F : \mathcal{D}(F) \subset L^2(0, t^{\text{end}}) \rightarrow L^2(0, t^{\text{end}})$ define the mapping which is given by

$$[F(G)](t) := u(l, t), \quad t \in [0, t^{\text{end}}], \quad (10)$$

where u denotes the solution of (6) – (8). Then we can rewrite the problem (9) as an operator equation

$$F(G) = u_{\text{data}}, \quad G \in \mathcal{D}(F). \quad (11)$$

The domain $\mathcal{D}(F)$ under consideration may contain all a priori information on the time-dependent behavior of G . In the simplest case we assume continuity and box constraints, i.e.

$$\mathcal{D}(F) := \mathcal{D}_{\text{box}} \cap L^2(0, t^{\text{end}}). \quad (12)$$

Furthermore, we restrict $\mathcal{D}(F)$ by known local monotonicity constraints on some subintervals to obtain additional stabilization of the inverse problem. The assumption that F maps into the space $L^2(0, t^{\text{end}})$ seems to be natural when we consider the numerical solution of (11) in a least-squares sense.

3 Well-posedness of the forward problem

In this section, we consider the continuous dependence of the solution of initial-boundary value problem (1) – (4) on the given gas temperature $G(t)$, $t \in [0, t^{\text{end}}]$. To simplify the analysis we assume that the coefficients C^A and κ do not depend on the temperature u . Note that the generalization of the considerations given below to the case of temperature-dependent coefficients is not difficult.

Let $G_1, G_2 \in \mathcal{D}_{\text{box}}$ be two given parameters, where $u_1 = u_1(x, t)$ and $u_2 = u_2(x, t)$ with $(x, t) \in \overline{Q}$ denote the corresponding solutions of (1) – (4). We set $h := G_2 - G_1$ and $w := u_2 - u_1$. In particular we have $h \in L^2(0, t^{\text{end}})$. Using the mean value theorem for functions of several variables we derive

$$f_{\text{rad}}(x, t, G_2(t), u_2(0, t)) - f_{\text{rad}}(x, t, G_1(t), u_1(0, t)) = \\ \frac{\partial}{\partial G} f_{\text{rad}}(x, t, \tilde{G}(x, t), \tilde{u}(x, t)) h(t) + \frac{\partial}{\partial D} f_{\text{rad}}(x, t, \tilde{G}(x, t), \tilde{u}(x, t)) w(0, t) =: f_{\text{rad}}^1(x, t)$$

for $(x, t) \in Q$ and two intermediate functions $\tilde{G}(x, t)$ and $\tilde{u}(x, t)$ satisfying

$$\min\{G_1(t), G_2(t)\} \leq \tilde{G}(x, t) \leq \max\{G_1(t), G_2(t)\}$$

and

$$\min\{u_1(0, t), u_2(0, t)\} \leq \tilde{u}(x, t) \leq \max\{u_1(0, t), u_2(0, t)\},$$

respectively, for $(x, t) \in Q$. Note that both intermediate functions $\tilde{G}(x, t)$ and $\tilde{u}(x, t)$ depend on t as well as on x . Hence for $w = w(x, t)$ we obtain the initial-boundary value problem

$$\left. \begin{aligned} C^A(x, t) \frac{\partial w(x, t)}{\partial t} - \frac{\partial}{\partial x} \left(\kappa(x) \frac{\partial w(x, t)}{\partial x} \right) &= f_{\text{rad}}^1(x, t), & (x, t) \in Q, \\ -\kappa(0) \frac{\partial w(0, t)}{\partial x} &= h_0 (h(t) - w(0, t)), & t \in [0, t^{\text{end}}], \\ \kappa(l) \frac{\partial w(l, t)}{\partial x} &= -h_s w(l, t), & t \in [0, t^{\text{end}}], \\ w(x, 0) &= 0, & x \in [0, l]. \end{aligned} \right\} \quad (13)$$

For the problem (13) we can apply the theory of linear parabolic equations, see e.g. [2, Chapter 7.1]. Therefore, we consider the weak formulation of this initial-boundary value problem. Let $H^1(0, l)$ be the Sobolev space of all functions $v \in L^2(0, l)$ with $v' \in L^2(0, l)$ with norm

$$\|v\|_{H^1(0, l)} := \left[\int_0^l v^2(x) dx + \int_0^l (v'(x))^2 dx \right]^{\frac{1}{2}},$$

while $(H^1(0, l))'$ denotes its dual space. We define $B : H^1(0, l) \times H^1(0, l) \times [0, t^{\text{end}}] \longrightarrow \mathbb{R}$ as the time-dependent bilinear form

$$B(\hat{w}, \hat{v}, t) := \int_0^l \kappa \frac{\partial \hat{w}}{\partial x} \frac{\partial \hat{v}}{\partial x} dx + h_0 \hat{w}(0) \hat{v}(0) + h_s \hat{w}(l) \hat{v}(l) - \hat{w}(0) \int_0^l \frac{\partial}{\partial D} f_{\text{rad}}(\tilde{G}, \tilde{u}) \hat{v} dx.$$

Moreover, let $f(t) : H^1(0, l) \longrightarrow \mathbb{R}$ denote the time-dependent functional defined by

$$\langle f(t), \hat{v} \rangle := h_0 \hat{v}(0) + \int_0^l \frac{\partial}{\partial G} f_{\text{rad}}(\tilde{G}, \tilde{u}) \hat{v} \, dx, \quad \hat{v} \in H^1(0, l).$$

Then, a function $w \in L^2(0, t^{\text{end}}; H^1(0, l))$ with $w_t \in L^2(0, t^{\text{end}}; (H^1(0, l))')$ and $w(x, 0) = 0$, $x \in [0, l]$, is called a weak solution of (13) if

$$\int_0^{t^*} \int_0^l C^A \frac{\partial w}{\partial t} \hat{v} \, dx \, dt + \int_0^{t^*} B(w(t), \hat{v}, t) \, dt = \int_0^{t^*} h(t) \langle f(t), \hat{v} \rangle \, dt \quad \forall \hat{v} \in L^2(0, t^{\text{end}}; H^1(0, l))$$

for almost all $t^* \in [0, t^{\text{end}}]$. Here, the norm of the space $L^2(0, t^{\text{end}}; H^1(0, l))$ of abstract functions is defined as

$$\|w\|_{L^2(0, t^{\text{end}}; H^1(0, l))} := \left[\int_0^{t^{\text{end}}} \left(\int_0^l w^2(x, t) \, dx + \int_0^l (w'(x, t))^2 \, dx \right) dt \right]^{\frac{1}{2}}.$$

The space $L^2(0, t^{\text{end}}; (H^1(0, l))')$ is defined analogously.

To apply well-known solvability results for weak solutions of parabolic problems, we have to assume that f_{rad} is differentiable with respect to G and D and

$$f_{\text{rad}}^D := \sup \left| \frac{\partial f_{\text{rad}}}{\partial D} \right| < \infty \quad \text{and} \quad f_{\text{rad}}^G := \sup \left| \frac{\partial f_{\text{rad}}}{\partial G} \right| < \infty \quad (14)$$

hold for $(x, t) \in Q_t$. This leads to the following proposition.

Proposition 3.1 *Assume that C^A and κ satisfy (5). Moreover, let $f_{\text{rad}}(x, t, G, D)$ be differentiable with respect to G and D and let (14) hold. Then, for every $h \in L^2(0, t^{\text{end}})$, the initial-boundary value problem (13) possesses a unique weak solution $w \in L^2(0, t^{\text{end}}; H^1(0, l))$ with*

$$\sup_{t \in (0, t^{\text{end}}]} \|w(\cdot, t)\|_{L^2(0, l)}^2 + \|w\|_{L^2(0, t^{\text{end}}; H^1(0, l))}^2 \leq C \|h\|_{L^2(0, t^{\text{end}})}^2. \quad (15)$$

SKETCH OF THE PROOF. Under the assumptions of the proposition there exist constants C_1, C_2 and C_3 which satisfy

$$|B(\hat{w}, \hat{v}, t)| \leq C_1 \|\hat{w}\|_{H^1(0, l)} \|\hat{v}\|_{H^1(0, l)}, \quad \forall \hat{w}, \hat{v} \in H^1(0, l),$$

and

$$B(\hat{w}, \hat{w}, t) + C_2 \|\hat{w}\|_{L^2(0, l)}^2 \geq C_3 \|\hat{w}\|_{H^1(0, l)}^2, \quad \forall \hat{w} \in H^1(0, l),$$

and almost all $t \in (0, t^{\text{end}}]$. In this context, these constants depend only on $l, \kappa_1, \kappa_2, h_0, h_s$ and f_{rad}^D . Moreover, the norm of the functional $f(t)$ is bounded by a constant C_4 which depends only on l, h_0 and f_{rad}^G . In particular, C_4 does not depend on t . Following the proofs of [2, Section 7.1, Theorems 3 and 4] we derive the existence of a unique weak solution w of (13), by noting that the cited results depend only on the properties of

the bilinear form $B(\tilde{w}, \tilde{v}, t)$ and not on the corresponding boundary conditions of (13). Moreover, the estimate

$$\begin{aligned} \sup_{t \in (0, t^{\text{end}}]} \|w(\cdot, t)\|_{L^2(0, l)}^2 + \|w\|_{L^2(0, T; H^1(0, l))}^2 &\leq \tilde{C} \int_0^{t^{\text{end}}} (h(t) \|f(t)\|_{(H^1(0, l))'})^2 dt \\ &\leq \tilde{C} C_4^2 \|h\|_{L^2(0, t^{\text{end}})}^2, \end{aligned}$$

holds by [2, Section 7.1, Theorem 2], which proves the theorem with $C := \tilde{C} C_4^2$. ■

Now we can directly conclude the uniqueness of the solution to (1) – (4) and the continuous dependence of this solution on the gas temperature function $G \in \mathcal{D}_{\text{box}}$.

Corollary 3.2 *The unique solution $u \in L^2(0, t^{\text{end}}; H^1(0, l))$ of (1) – (4) depends continuously on the gas temperature function $G \in \mathcal{D}_{\text{box}}$. In particular, for $G_1, G_2 \in \mathcal{D}_{\text{box}}$ and corresponding solutions u_1 and u_2 , respectively, of (1) – (4) we have the estimate*

$$\|u_2 - u_1\|_{L^2(0, t^{\text{end}}; H^1(0, l))} \leq C \|G_2 - G_1\|_{L^2(0, t^{\text{end}})} \quad (16)$$

with a constant $C > 0$ that does not depend on G_1 and G_2 .

PROOF. The continuous dependence of the solution u on the parameter function G follows directly as a consequence of the estimate (15). Let $G \in \mathcal{D}_{\text{box}}$ be given arbitrarily and let u and \tilde{u} be two solutions of (1) – (4). Then $w := u - \tilde{u}$ satisfies (13) with $h \equiv 0$. From Proposition 3.1 we then have $w \equiv 0$ and hence $u \equiv \tilde{u}$. ■

4 Numerical approximation of the forward problem

In this section, we outline the approximate numerical solution of the initial-boundary value problem (1) – (4). Here, the gas temperature $G(t)$ is assumed to be known. The time- and space-dependence and the nonlinearities in C^A , κ and f_{rad} require some special treatment.

We are going to use as time-stepping algorithm the classical backward Euler scheme: Let τ denote the time increment and $u^n(x)$ the approximate solution at time step t_n , then for $t_{n+1} = t_n + \tau$ we have to solve the nonlinear (ordinary) differential equation

$$C^A(x, t_{n+1}, u^{n+1}) \frac{u^{n+1} - u^n}{\tau} - \frac{d}{dx} \left(\kappa(x, u^{n+1}) \frac{d}{dx} u^{n+1} \right) = f_{\text{rad}}(x, t_{n+1}, G(t_{n+1}), u^{n+1}(0)) \quad (17)$$

for $x \in (0, l)$ in space with boundary conditions

$$\begin{aligned} -\kappa(0, u^{n+1}(0)) \frac{d}{dx} u^{n+1}(0) &= h_0 (G(t_{n+1}) - u^{n+1}(0)), \\ \kappa(l, u^{n+1}(l)) \frac{d}{dx} u^{n+1}(l) &= -h_s u^{n+1}(l). \end{aligned}$$

For the discretization in space, we can use linear finite elements. Here, the fact of one space dimension leads to stiffness and mass matrices that are tridiagonal and each linear system

with such a matrix is solved with optimal arithmetical complexity (proportional to the number of unknowns). So, we can use a very fine mesh without concerns of computational time. For this reason it seems to be convenient to focus on linear elements. Let $x_i = i h$ be the discretization points and $\varphi_i(x)$ the hat-functions (linear in each interval $[x_{i-1}, x_i]$ and $\varphi_i(x_j) = \delta_{ij}$) with $h = l/N$ and $i = 0, \dots, N$. The equidistance of the points x_i is not necessary. Then, the weak formulation of (17) reads as:

Find $u^{n+1}(x) \in H^1(0, l)$ with

$$\begin{aligned} \langle C^A u^{n+1}, v \rangle_x + \tau \left\langle \kappa \frac{\partial}{\partial x} u^{n+1}, \frac{\partial}{\partial x} v \right\rangle_x + \tau v(0) h_0 u^{n+1}(0) + \tau v(l) h_s u^{n+1}(l) \\ = \tau \langle f, v \rangle_x + \langle C^A u^n, v \rangle_x + v(0) \tau h_0 G(t_{n+1}) \quad \forall v \in H^1(0, l). \end{aligned} \quad (18)$$

Here, $\langle u, v \rangle_x = \int_0^l u v dx$ stands for the L_2 -inner product of functions over $[0, l]$. Note that $C^A := C^A(x, t_{n+1}, u^{n+1})$, $\kappa := \kappa(x, u^{n+1})$ and $f := f_{\text{rad}}(x, t_{n+1}, G(t_{n+1}), u^{n+1}(0))$ contain the nonlinearities associated with their dependence on the solution u^{n+1} at the current time step.

With $u^{n+1}(x) = \sum_{i=0}^N u_i^{n+1} \varphi_i(x)$ we represent the finite element approximation of this function by a unique vector $\underline{u}^{n+1} = (u_i^{n+1})_{i=0}^N \in \mathbb{R}^{N+1}$. Then (18) coincides approximately with the non-linear system of $N + 1$ equations

$$M(\underline{u}^{n+1}) \underline{u}^{n+1} + \tau K(\underline{u}^{n+1}) \underline{u}^{n+1} = \tau \underline{b}(\underline{u}^{n+1}) + M(\underline{u}^{n+1}) \underline{u}^n \quad (19)$$

with the tridiagonal matrices M and K , which depend on the solution as

$$\begin{aligned} M(\underline{u}) &= \left(\langle C^A(x_j, t_{n+1}, u_j) \varphi_j, \varphi_i \rangle_x \right)_{i,j=0}^N, \\ K(\underline{u}) &= \left(\left\langle \kappa(x_j, u_j) \frac{\partial}{\partial x} \varphi_j, \frac{\partial}{\partial x} \varphi_i \right\rangle_x + h_0 \varphi_j(0) \varphi_i(0) + h_s \varphi_j(l) \varphi_i(l) \right)_{i,j=0}^N \end{aligned}$$

and

$$\underline{b}(\underline{u}) = (\langle f_{\text{rad}}(x_i, t_{n+1}, G(t_{n+1}), u_0), \varphi_i \rangle_x + \varphi_i(0) h_0 G(t_{n+1}) + \varphi_i(l) h_s T_{\text{amb}})_{i=0}^N.$$

To solve equation (19) we consider the convergence of the iteration

$$\begin{aligned} \underline{v}^{(0)} &:= \underline{u}^n, \quad \underline{v}^{(k)} \text{ is the solution of} \\ (M(\underline{v}^{(k-1)}) + \tau K(\underline{v}^{(k-1)})) \underline{v} &= \tau \underline{b}(\underline{v}^{(k-1)}) + M(\underline{v}^{(k-1)}) \underline{u}^n \quad k = 1, 2, \dots \end{aligned} \quad (20)$$

We can prove convergence of the iteration process (20).

Lemma 4.1 *Let C^A , κ and f_{rad} be differentiable functions with respect to u and let their derivatives remain bounded. Then there exists a constant τ_0 such that the iteration process (20) converges to the unique solution of (19) for all $0 < \tau < \tau_0$.*

SKETCH OF A PROOF. We can rewrite (19) as a fixed-point equation as follows

$$\begin{aligned} \underline{u} &= (M(\underline{u}) + \tau K(\underline{u}))^{-1} (\tau \underline{b}(\underline{u}) + M(\underline{u}) \underline{u}^n) \\ &= (M(\underline{u}) + \tau K(\underline{u}))^{-1} (\tau \underline{b}(\underline{u}) + (M(\underline{u}) + \tau K(\underline{u})) \underline{u}^n - \tau K(\underline{u}) \underline{u}^n) \\ &= \tau (M(\underline{u}) + \tau K(\underline{u}))^{-1} (\underline{b}(\underline{u}) - K(\underline{u}) \underline{u}^n) + \underline{u}^n \\ &=: T(\underline{u}) \end{aligned}$$

with the nonlinear operator $T : \mathbb{R}^{N+1} \longrightarrow \mathbb{R}^{N+1}$. Let be $\underline{u}_1, \underline{u}_2 \in \mathbb{R}^{N+1}$. Under the conditions stated above we can use Taylor's expansion to derive the estimate

$$\|T(\underline{u}_1) - T(\underline{u}_2)\|_2 \leq \tau C \|\underline{u}_1 - \underline{u}_2\|_2$$

with a constant $C > 0$ chosen independently of \underline{u}_1 and \underline{u}_2 . Here, $\|\cdot\|_2$ denotes the Euclidean norm. Choosing the time step τ sufficiently small, i.e. $\tau < \tau_0 := C^{-1}$, the mapping T is contractive. Hence, equation (19) has a unique solution \underline{u}^{n+1} and we obtain convergence $\underline{u}^{(k)} \rightarrow \underline{u}^{n+1}$ as $k \rightarrow \infty$. ■

Note that discontinuities with respect to u occur in the original problem (1) – (4) in the coefficient C^A caused by the modelled effects of moisture evaporation and thermochemical processes inside the textile (see [12]). On the other hand, numerical tests have shown that such jumps in the parameters can destroy the convergence of the iteration process (20). Therefore, discontinuous coefficients have to be approximated by sufficiently smooth functions. We have successfully used an approximation of C^A with piecewise linear functions in temperature.

5 Properties of the Calibration problem

For solving the inverse problem (11) by an appropriate algorithm we have to consider the differentiability of the operator F . Therefore, let $G_0, G_1 \in \mathcal{D}(F)$ be given arbitrarily and set $h := G_1 - G_0$. Moreover let, for $\varepsilon \in [0, 1]$, u_ε denote the solution of (6) – (8) with $G_0 + \varepsilon h$ instead of G . Furthermore, for $\varepsilon > 0$, we set $z_\varepsilon := \frac{1}{\varepsilon}(u_\varepsilon - u_0)$. Then z_ε is the solution of the initial-boundary value problem (6) – (8) when f_{rad} is replaced by

$$\frac{\partial}{\partial G} f_{\text{rad}}(x, t, \hat{G}_\varepsilon(x, t), \hat{u}_\varepsilon(x, t)) h(t) + \frac{\partial}{\partial D} f_{\text{rad}}(x, t, \hat{G}_\varepsilon(x, t), \hat{u}_\varepsilon(x, t)) z_\varepsilon(0, t)$$

with two intermediate functions $\hat{G}_\varepsilon(x, t)$ and $\hat{u}_\varepsilon(x, t)$ for $(x, t) \in Q$. Hence z_ε exists for every $\varepsilon > 0$. Moreover, we have $\hat{G}_\varepsilon(x, t) \rightarrow G_0(t)$ and $\hat{u}_\varepsilon(x, t) \rightarrow u_0(0, t)$ for $\varepsilon \rightarrow 0$. By considering the limit $z := \lim_{\varepsilon \rightarrow 0} z_\varepsilon$ it follows now easily that $z = z(x, t)$ is the solution of

$$\left. \begin{aligned} C_{\text{Cu}} \frac{\partial z}{\partial t} - \kappa_{\text{Cu}} \frac{\partial^2 z}{\partial x^2} &= \hat{f}_{\text{rad}}(x, t), & (x, t) \in Q, \\ -\kappa_{\text{Cu}} \frac{\partial z(0, t)}{\partial x} &= h_0(h(t) - z(0, t)), & t \in (0, t^{\text{end}}], \\ \kappa_{\text{Cu}} \frac{\partial z(l, t)}{\partial x} &= -h_s z(l, t), & t \in (0, t^{\text{end}}], \\ z(x, 0) &= 0, & x \in [0, l], \end{aligned} \right\} \quad (21)$$

with

$$\hat{f}_{\text{rad}}(x, t) := \frac{\partial}{\partial G} f_{\text{rad}}(x, t, G_0(t), u_0(0, t)) h(t) + \frac{\partial}{\partial D} f_{\text{rad}}(x, t, G_0(t), u_0(0, t)) z(0, t).$$

Moreover, we have

$$\frac{\partial}{\partial G} f_{\text{rad}}(x, t, G, D) = 4 \gamma e^{-\gamma x} \beta_{\text{Gas}} (G + T_0)^3 =: f_1(x, t) \quad (22)$$

and

$$\frac{\partial}{\partial D} f_{\text{rad}}(x, t, G, D) = -4 \gamma e^{-\gamma x} \beta_{\text{Obj}} (D + T_0)^3 =: f_2(x, t). \quad (23)$$

Replacing f_{rad}^1 by \hat{f}_{rad} we can derive analogous to Proposition 3.1 the following existence result.

Lemma 5.1 *Let be $G_0 \in \mathcal{D}_{\text{box}}$ and the conditions of Proposition 3.1 hold. Then, for every $h \in L^2(0, t^{\text{end}})$, the initial-boundary value problem (21) possesses a unique weak solution $z \in L^2(0, t^{\text{end}}; H^1(0, l))$ with*

$$\sup_{t \in (0, t^{\text{end}}]} \|z(\cdot, t)\|_{L^2(0, l)}^2 + \|z\|_{L^2(0, t^{\text{end}}; H^1(0, l))}^2 \leq C \|h\|_{L^2(0, t^{\text{end}})}^2 \quad (24)$$

for some constant $C > 0$.

Now we can prove differentiability of the operator F .

Proposition 5.2 *Let $\mathcal{X} = L^2(0, t^{\text{end}})$. Then the operator F is Gâteaux-differentiable in $\mathcal{D}(F)$. For given $G_0 \in \mathcal{D}(F)$ the Gâteaux-derivative $F'(G_0) : L^2(0, t^{\text{end}}) \rightarrow L^2(0, t^{\text{end}})$ is given by*

$$[F'(G_0) h](t) := z(l, t), \quad t \in (0, t^{\text{end}}), \quad (25)$$

where z is the solution of (21). Moreover, the norm of the derivative is uniformly bounded.

PROOF. Let $G_0, G_1 \in \mathcal{D}(F)$ with $h := G_1 - G_0$ and u_ε defined as above. Then

$$[F'(G_0) h](t) := \lim_{\varepsilon \rightarrow 0} \frac{[F(G_0 + \varepsilon h)](t) - [F(G_0)](t)}{\varepsilon} = \lim_{\varepsilon \rightarrow 0} \frac{u_\varepsilon(l, t) - u_0(l, t)}{\varepsilon} = z(l, t)$$

for $t \in (0, t^{\text{end}})$. Hence (25) defines the directional derivative of F in G_0 in the direction h . By Lemma 5.1 the definition can be extended to arbitrary $h \in L^2(0, t^{\text{end}})$. Obviously $F'(G_0)$ is a linear operator and by estimate (24) we obtain

$$\begin{aligned} \|F'(G_0) h\|_{L^2(0, t^{\text{end}})}^2 &= \int_0^{t^{\text{end}}} (z(l, t))^2 dt \leq C \int_0^{t^{\text{end}}} \|z(\cdot, t)\|_{H^1(0, l)}^2 dt \\ &= C \|z\|_{L^2(0, t^{\text{end}}; H^1(0, l))}^2 \leq C \|h\|_{L^2(0, t^{\text{end}})}^2, \end{aligned}$$

with constant $C > 0$ independent of G_0 . Here we use the fact that the mapping $\tilde{z} \in H^1(0, l) \mapsto \tilde{z}(l)$ is a bounded functional in $H^1(0, l)$. ■

For finding least-squares solutions of (11) iteratively, we also need the adjoint operator $F'(G_0)^* : L^2(0, t^{\text{end}}) \rightarrow L^2(0, t^{\text{end}})$ of $F'(G_0)$. Therefore we define $w = w(x, t)$, $(x, t) \in \overline{Q}$, as solution of the problem

$$\left. \begin{aligned} -C_{\text{Cu}} \frac{\partial w}{\partial t} &= \kappa_{\text{Cu}} \frac{\partial^2 w}{\partial x^2}, & (x, t) \in Q, \\ -\kappa_{\text{Cu}} \frac{\partial w(0, t)}{\partial x} &= -h_0 w(0, t) + \int_0^l f_2(x, t) w(x, t) dx, & t \in [0, t^{\text{end}}], \\ \kappa_{\text{Cu}} \frac{\partial w(l, t)}{\partial x} &= -h_s w(l, t) + p(t), & t \in [0, t^{\text{end}}], \\ w(x, t^{\text{end}}) &= 0, & x \in [0, l], \end{aligned} \right\} \quad (26)$$

Then the following result holds.

Proposition 5.3 *The adjoint operator $F'(G_0)^* : L^2(0, t^{\text{end}}) \longrightarrow L^2(0, t^{\text{end}})$ of the Gâteaux-derivative $F'(G_0)$ is given by*

$$[F'(G_0)^* p](t) := \int_0^l f_1(x, t) w(x, t) dx + h_0 w(0, t), \quad t \in (0, t^{\text{end}}),$$

for arbitrary $p \in L^2(0, t^{\text{end}})$, where w denotes the solution of (26).

The proof is omitted here, because it is a straightforward calculation to show that

$$\int_0^{t^{\text{end}}} [F'(G_0) h](t) p(t) dt = \int_0^{t^{\text{end}}} h(t) [F'(G_0)^* p](t) dt$$

for all admissible parameters $h, p \in L^2(0, t^{\text{end}})$, where $F'(G_0)^*$ is defined as above.

6 Solution approaches for the inverse problem

For the inverse problem aimed at finding the gas temperature $G(t)$, $t \in [0, t^{\text{end}}]$, real measurements $u_{\text{data}}(t)$, $t \in [0, t^{\text{end}}]$, can be exploited as data (see Figure 3), where the simplified version of the arc test without additional textile material was performed for providing such data. The used constants based on the technological literature (for details see also [11] and [12]) are specified by the following list:

$$\begin{aligned} l &= 1.6 \text{ mm}, \\ \kappa_{\text{Cu}} &= 392 \text{ W} \cdot \text{m}^{-1} \text{ K}^{-1}, \\ C_{\text{Cu}} &= 3.4265 \cdot 10^6 \text{ J} \cdot \text{m}^{-3} \text{ K}^{-1}, \\ \gamma &= 2.05 \cdot 10^5 \text{ m}^{-1}, \\ q_a(t) &= 7.055 \cdot 10^4 \text{ W} \cdot \text{m}^{-2} \cdot \chi_{[0, t_p]}(t), \\ \beta_{\text{Gas}} &= 1.114 \cdot 10^{-9} \text{ W} \cdot \text{m}^{-2} \text{ K}^{-4}, \\ \beta_{\text{Obj}} &= 4.72 \cdot 10^{-8} \text{ W} \cdot \text{m}^{-2} \text{ K}^{-4}, \\ h_0 &= 40 \text{ W} \cdot \text{m}^{-2} \text{ K}^{-1}, \\ h_s &= 15 \text{ W} \cdot \text{m}^{-2} \text{ K}^{-1}. \end{aligned}$$

Here, $\chi_{[a, b]}$ is the characteristic function with respect to the interval $[a, b]$. The values β_{Gas} and β_{Obj} are products of dimensionless factors with the Stefan-Boltzmann constant. The domain $\mathcal{D}(F)$ is given by (12) and a maximal temperature $G_{\text{max}} = 8000 \text{ K}$.

Determination without regularization

Since the calibration problem is a nonlinear inverse problem with smoothing forward operator F , local ill-posedness in the sense of [6, Def. 2] must be expected. For studying the ill-posedness effects occurring with equation (11) we first test a discretized version of the least-squares fitting

$$\|F(G) - u_{\text{data}}\|_{L^2(0, t^{\text{end}})}^2 \longrightarrow \min, \quad \text{subject to} \quad G \in \mathcal{D}(F). \quad (27)$$

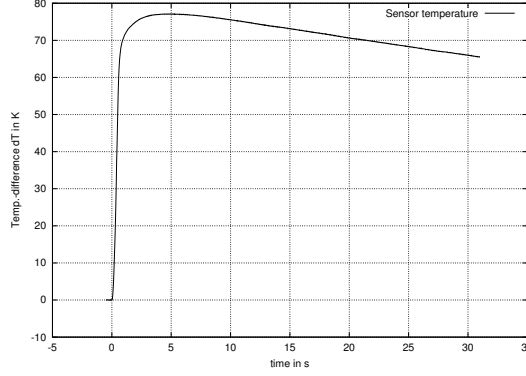


Figure 3: Calibration measurements of calorimeter temperature.

We suggest a Newton-CG algorithm for solving the problem (27). Let $G_0 \in \mathcal{D}(F)$ be an initial guess. Then the classical Gauß-Newton algorithm reads as $G_{j+1} := G_j + h_j$, $j = 0, 1, \dots$, where the increment h_j denotes the solution of linear normal equation

$$F'(G_j)^* F'(G_j) h = F'(G_j)^* (u_{\text{data}} - F(G_j)). \quad (28)$$

Based on the knowledge of $F'(G_j)$ and $F'(G_j)^*$ we can use a CGLS-algorithm for solving (28) (see, e.g., [1, Section 7.1]).

The Newton-CG algorithm is a modification of (28). The Newton step h_j is not calculated exactly, but approximated by the K -th CG iteration step $h_{j,K}$. The stopping index $K = K(j)$ is chosen by an appropriate stopping criterion. For example we can choose K as smallest index which satisfies

$$\|F(G_j) + F'(G_j) h_{j,K} - u_{\text{data}}\| \leq \max \{ \eta \|F(G_j) - u_{\text{data}}\|, \text{TOLMIN} \} \quad (29)$$

for a constant $0 < \eta < 1$ and a minimal tolerance TOLMIN. Choosing η not too small leads to a stabilization (regularization) of the algorithm (see [3]). Additionally, we have to ensure, that $G_{j+1} \in \mathcal{D}(F)$. For this reason, a projection onto $\mathcal{D}(F)$ might be added in the algorithm.

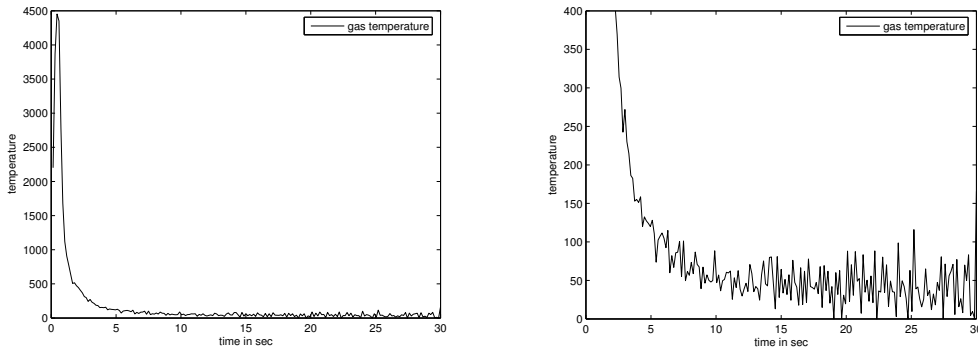


Figure 4: Gas temperature without regularization with zoom in the lower temperature interval.

A solution G_{ls} of the extremal problem (27) for our data u_{data} is shown in Figure 4. The peak of $G_{ls}(t)$ in a neighborhood of $t \approx t_p = 0.5s$ caused by the extreme energy

of the electric arc seems to be approximated quite well. For times t after this peak a temperature decay (first with a high and at the end with a low rate) occurs, but there we find strong oscillations of G_{ls} in the cooling phase, which are not physically interpretable and obviously express ill-posedness phenomena. Such oscillations cannot be accepted in the approximate solution of G for practical use, since forward computations of the arc test with real textile materials seem to be more sensitive to gas temperature changes in the final phase of cooling. This is due to the fact that the thermal conductivity of the isolation material is much lower than in the simplified test situation used for solving the inverse problem.

A Tikhonov regularization approach

In order to overcome the drawback of ill-posedness, we should follow a regularization approach (cf., e.g., [1], [5]) for solving the operator equation (11) by a numerical procedure (see also [15]). Next instead of (27) we use a discretized version of the second order standard Tikhonov method solving the extremal problem

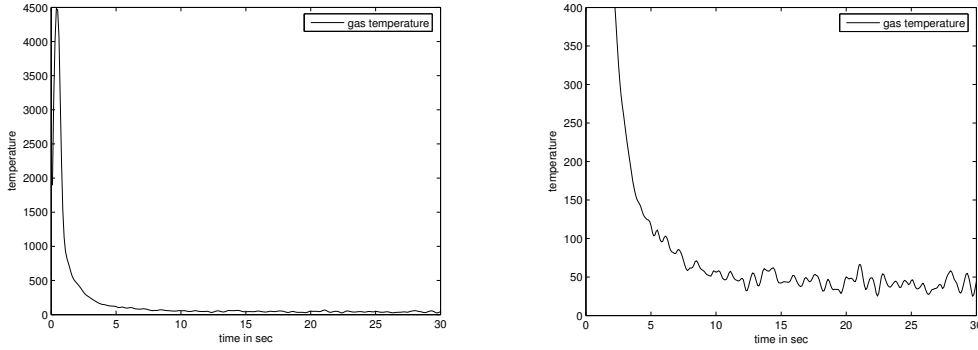


Figure 5: Gas temperature with second order Tikhonov regularization and zoom.

$$\|F(G) - u_{\text{data}}\|_{L^2(0, t_{\text{end}})}^2 + \alpha \|G''\|_{L^2(0, t_{\text{end}})}^2 \longrightarrow \min, \quad \text{subject to } G \in \mathcal{D}(F), \quad (30)$$

with minimizer G_α . For existence and stability of such minimizers G_α for all $\alpha > 0$ we refer, for example, to [8]. Note, that the term $\|G''\|_{L^2(0, t_{\text{end}})}^2$ leads to a stronger penalization of the oscillations in the solution than the standard Tikhonov approach $\|G\|_{L^2(0, t_{\text{end}})}^2$. Another reason for avoiding the latter term can be found in the structure of the solution. Penalization of the norm of the solution would flatten the peak in the gas temperature curve. Again we used a Newton-CG algorithm for solving the minimization problem (30). It can be done similarly to the least-squares fitting stated above. However, the normal equation (28) has to be replaced by the normal equation

$$(F'(G_j)^* F'(G_j) + \alpha L^* L) h = F'(G_j)^* (u_{\text{data}} - F(G_j)) - \alpha L^* G_j \quad (31)$$

of the Tikhonov functional (30), where the linear differential operator $L : \mathcal{D}(L) \subset L^2(0, t_{\text{end}}) \longrightarrow L^2(0, t_{\text{end}})$ is defined as $L G := G''$ with domain $\mathcal{D}(L) := \{G \in L^2(0, t_{\text{end}}) : G'' \in L^2(0, t_{\text{end}})\}$.

In our studies the selection of the regularization parameter $\alpha > 0$ was performed based on the quasi-optimality criterion (see, e.g., [4, p.182]). It says that we choose the regularization parameter α as the minimum point of the functional $\|\alpha \frac{dG_\alpha}{d\alpha}\|$ for $\alpha \in (\alpha_{\min}, \alpha_{\max})$. Given a sequence of parameters $\alpha_i = q^i \alpha_0$ with $\alpha_0 = \alpha_{\max}$ and $0 < q < 1$ the minimization can be done approximately by choosing $\alpha = \alpha_i$ such that $\|G_{\alpha_{i+1}} - G_{\alpha_i}\|_{L^2(0, t^{\text{end}})}$ is minimal. The resulting quasi-optimal function G_α is shown in Figure 5. Oscillations also occur in the cooling phase, but they are less and much smaller compared to the least-squares fitting. Note that the image function $F(G_\alpha)$ for the regularized solution is still a good approximation of the data function u_{data} . The obtained regularization parameter α and the relative error of the approximation can be found in Table 1.

We know the basic theoretical drawback (see, e.g., [1, Theorem 3.3]) of criteria for choosing the regularization parameter α that do not exploit the noise level δ satisfying $\|u_{\text{exact}} - u_{\text{data}}\|_{L^2(0, t^{\text{end}})} \leq \delta$, but unfortunately the rapidly increasing temperature of the calorimeter (see Figure 3) in connection with temperatures up to 5000K near the arc and unknown inertia of the measurement system makes the prescription of a realistic δ required for the use of a discrepancy principle very problematic. On the other hand, the successful use of the quasi-optimality principle has been presented in very different practical applications in literature.

A descriptive regularization approach

As third approach we use an ansatz of descriptive regularization. In detail, we add more a priori information about the qualitative behavior of the gas temperature function, in particular the knowledge of monotonicity expressed by a more restricted domain $\mathcal{D}_{\text{descr}} \subset \mathcal{D}(F)$. During the burning time of the electric arc $t \in [0, t_p]$ we can assume a strictly growing function $G(t)$. On the other hand, for sufficiently large t , here $t \geq 2t_p$, we have a monotone decay of the gas temperature. For the gap interval $t \in (t_p, 2t_p)$ we do not impose additional requirements, but even for regularized solutions without monotonicity we have no oscillations in this time interval. Therefore, we define

$$\mathcal{D}_{\text{descr}} := \{G \in \mathcal{D}(F) : G(t) \text{ monotonically decreasing for } t \in [2t_p, t^{\text{end}}]\}.$$

The regularized solution G_α^{descr} presented in Figure 6 is obtained by solving a discretized version of

$$\|F(G) - u_{\text{data}}\|_{L^2(0, t^{\text{end}})}^2 + \alpha \|G''\|_{L^2(0, t^{\text{end}})}^2 \longrightarrow \min, \quad \text{subject to} \quad G \in \mathcal{D}_{\text{descr}} \quad (32)$$

again based on a quasi-optimal choice of the regularization parameter α . The numerical realization was performed by a penalty method. The values $G_\alpha^{\text{descr}}(t)$ of this approximate solution are not very different from the values $G_\alpha(t)$ for small t , but by construction the function $G_\alpha^{\text{descr}}(t)$ suppresses oscillations nearly complete. Since the approximation error of u_{data} by $F(G_\alpha^{\text{descr}})$ (see Table 1) is nearly the same as for Tikhonov regularization, the solution $G_\alpha^{\text{descr}}(t)$ seems to be the best approximation of the real gas temperature.

A numerical case study with synthetic data

To illustrate the results obtained we finally present a case study based on synthetic data. We consider the function

$$G^*(t) := \begin{cases} 125(4 - (t - 2)^2), & t \leq 3, \\ 345 \exp\left(\frac{3-t}{4}\right) + 30, & t > 3, \end{cases}$$

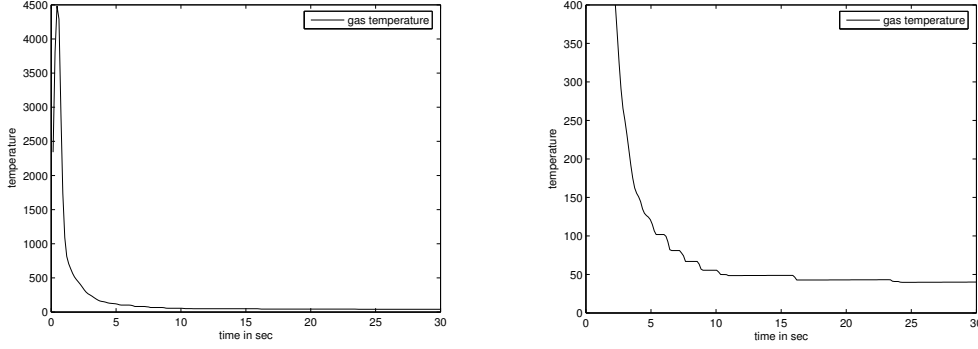


Figure 6: Gas temperature with descriptive regularization and zoom.

	α	$\frac{\ F(G_\alpha) - u_{\text{data}}\ }{\ u_{\text{data}}\ }$
Without regularization	—	$1.1082 \cdot 10^{-4}$
Tikhonov regularization	$2.2528 \cdot 10^{-6}$	$9.7514 \cdot 10^{-4}$
Descriptive regularization	$3.4337 \cdot 10^{-6}$	$1.113 \cdot 10^{-3}$

Table 1: Regularization parameters and relative data discrepancy values

to be determined on the interval $[0, t^{\text{end}}]$ with chosen $t^{\text{end}} = 30 \text{ s}$ again. Note that $G^*(t)$ has a similar structure as the gas temperature for the real data, but with a much lower peak at the beginning of the time interval. As data u_{data} we used a perturbation of the exact solution $F(G^*)$, where $\delta = 10^{-4}$ and $\delta = 10^{-3}$ denote the relative size of the added perturbations. In Tables 2 and 3 we present the corresponding numerical results. It can be seen in Table 2 that without regularization a relative error of 0.1 % in the data leads to a relative error of about 15 % in the solution, which shows the ill-posedness of the calibration problem. Using one of the two suggested regularization approaches for finding regularized solutions G_α we can stabilize the problem. However, the idea of descriptive regularization provides for both noise levels a better approximation of G^* .

In Table 2 the regularization parameter α is chosen by the quasi-optimality criterion. For a comparison, the final Table 3 also presents the results obtained by using Morozov's discrepancy principle for Tikhonov regularization. Since we know the absolute noise level δ_{abs} for the synthetic data, we can apply the discrepancy principle which recommends to choose $\alpha = \alpha(\delta_{abs})$ such that $\|F(G_\alpha) - u_{\text{data}}\| = \delta_{abs}$. We see that for both (relative) noise levels $\delta = 10^{-4}$ and $\delta = 10^{-3}$ the discrepancy principle provides a larger regularization parameter α and a worse approximation G_α of G^* than the quasi-optimality criterion. This can be explained by the well-known overregularization effect of the discrepancy method. On the other hand, we see that the quasi-optimality criterion seems to be a good alternative for choosing the regularization parameter whenever the noise level δ is unknown.

	Without regularization	Tikhonov regularization		Descriptive regularization	
δ	$\frac{\ G_\alpha - G^*\ }{\ G^*\ }$	α	$\frac{\ G_\alpha - G^*\ }{\ G^*\ }$	α	$\frac{\ G_\alpha - G^*\ }{\ G^*\ }$
0	$6.7512 \cdot 10^{-5}$	—	—	—	—
10^{-4}	0.0266	$1.1973 \cdot 10^{-6}$	0.0056	$9.6977 \cdot 10^{-7}$	0.0046
10^{-3}	0.1475	$4.2391 \cdot 10^{-4}$	0.0152	$3.4337 \cdot 10^{-4}$	0.0136

Table 2: Comparison of different solution approaches

	Morozov's discrepancy method		Quasi-optimality criterion	
	α	$\frac{\ G_\alpha - G^*\ }{\ G^*\ }$	α	$\frac{\ G_\alpha - G^*\ }{\ G^*\ }$
$\delta = 10^{-4}$	$2.8243 \cdot 10^{-5}$	0.0112	$1.1973 \cdot 10^{-6}$	0.0056
$\delta = 10^{-3}$	$1.668 \cdot 10^{-3}$	0.0202	$4.2391 \cdot 10^{-4}$	0.0152

Table 3: Comparison of different parameter choice strategies

7 Conclusions

- For a computer-based simulation of electric fault arc tests the determination of time-dependent gas temperature functions $G = G(t)$ near the arc has to be realized. This function cannot be measured directly because of high temperatures and therefore it has to be calibrated by using indirect measurements based on temperatures u sufficiently far away from the arc.
- In order to overcome the drawback of ill-posedness phenomena occurring in the corresponding nonlinear inverse problem of calibrating G , a regularization approach is required. Otherwise, strongly oscillating solutions are obtained which cannot be interpreted physically.
- Second order Tikhonov regularization provides acceptable approximate solutions G_α of G for the calibration problem when the regularization parameter $\alpha > 0$ is chosen by the quasi-optimality criterion.
- The solution can further be stabilized and improved by using ideas of descriptive regularization, i.e., by exploiting the partial monotonicity of expected solutions.

References

- [1] Engl, H.W.; Hanke, M.; Neubauer, A.: *Regularization of Inverse Problems*, Kluwer, Dordrecht 1996.
- [2] Evans, C.: *Partial Differential Equations*, AMS, Providence 1998.
- [3] Hanke, M.: *Regularizing properties of a truncated Newton-CG algorithm for nonlinear inverse problems*, Numer. Func. Anal. Optim. 18 (1997), 971–993.

- [4] Hansen, P.C.: *Rank-Deficient and Discrete Ill-Posed Problems*, SIAM, Philadelphia 1998.
- [5] Hofmann, B.: *Regularization for Applied Inverse and Ill-Posed Problems*, Teubner, Leipzig 1986.
- [6] Hofmann, B.; Scherzer, O.: *Factors influencing the ill-posedness of nonlinear problems*, Inverse Problems 10 (1994), 1277–1297.
- [7] Jakob, M.: *Heat Transfer*, Volume I, John Wiley & Sons, New York 1949.
- [8] Kunisch, K.; Ring, W.: *Regularization of nonlinear ill-posed problems with closed operators*, Numer. Funct. Anal. Optimization 14 (1993), No. 3-4, 389–404.
- [9] International Social Security Association (ISSA), Section Electricity–Gas–Long-Distance Heating–Water, *Guideline for the selection of personal protective clothing when exposed to the thermal effects of an electric arc*, c/o Berufsgenossenschaft der Feinmechanik und Elektrotechnik, Köln 2002.
- [10] Ladyženskaja, O.A.; Solonnikov, V.A.; Ural'ceva, N.N.: *Linear and Quasilinear Equations of Parabolic Type*, American Mathematical Society, Providence, Rhode Island 1968.
- [11] Schau, H.; Haase, J.: *Electric fault arc calorimetric analysis based on ENV 50354:2000*. Proceedings of the 6th International Conference on Live Maintenance (ICOLIM 2002) , VDE-Verlag, Berlin 2002, pp.333-339.
- [12] Steinhorst, P.: *Simulation of the Nonstationary Heat Transfer Through Heat Protecting Textiles* (in German). Diploma Thesis, Faculty of Mathematics, Chemnitz University of Technology, Chemnitz 2003.
- [13] Steinhorst, P.; Hofmann, B.; Meyer, A.; Weinelt, W.: *Gas temperature identification for the simulation of electric fault arc tests*, In: 5th International Conference on Inverse Problems in Engineering: Theory and Practice, Cambridge 11-15 July 2005, Volume III, Ed.: D. Lesnic. Leeds University Press, Leeds UK 2005, pp. S12/1–8.
- [14] Torvi, D.A.; Dale, J.D.: *Heat transfer in thin fibrous materials under high heat flux*, Fire Technology 35 (1999), No.3, 210–231.
- [15] Vogel, C.R.: *Computational Methods for Inverse Problems*, SIAM, Philadelphia 2002.
- [16] Zeidler, E.: *Nonlinear Functional Analysis and its Applications I – Fixed-Point Theorems*, Springer, New York 1985.